A Percentile Based ADR for Mobile LoRaWAN Applications

Geraldo A. Sarmento Neto[1], Thiago A. R. Silva[1,2], Pedro F. F. Abreu[1], Arthur F. S. Veloso[1], Luis H. O. M[1], José Valdemir R. Junior[1]

[1]Federal University of Piauí (UFPI), Teresina – PI – Brazil

[2]Federal Institute of Maranhão (IFMA), Barra do Corda – MA – Brazil

{geraldosarmento,thiago.allisson,pedroffda

arturfdasveloso,luishenriqueom,valdemirreis}@ufpi.edu.br

Abstract. *The article presents a novel solution addressing the limitations of Adaptive Data Rate (ADR) mechanism in LoRaWAN networks, particularly in scenarios characterized by fluctuating channel conditions. By employing percentile-based statistical techniques, the proposed P-ADR optimizes Signal-to-Noise Ratio (SNR) estimation for adjusting transmission parameters, thereby enhancing reliability while preserving energy efficiency. Simulation results revealed superior performance of P-ADR, exhibiting an average Packet Delivery Ratio (PDR) advantage of approximately 5% over ADR+ and around 25% over standard ADR in mobile scenarios. The outcome highlights P-ADR potential as a viable and efficient alternative, improving reliability in LPWAN applications.*

1. Introduction

The Internet of Things (IoT) has emerged as a communication paradigm aimed at interconnecting devices to the Internet, enabling real-time data collection and processing. This large-scale interconnection promotes the creation of an intelligent ecosystem where devices can be monitored, controlled, and integrated into complex systems [Sadhu et al. 2022]. The versatility of IoT allows the development of applications in various sectors such as smart agriculture, environmental monitoring, smart cities, smart meters for energy and water consumption, and smart health. For instance, sensors can gather data on soil moisture and climate, enabling precision agriculture with efficient resource utilization [Jouhari et al. 2023].

In this context, Low-Power Wide-Area Network (LPWAN) technologies arise as a promising solution for IoT applications. This network category is designed to meet the specific requirements of IoT devices, offering extended range, minimized energy consumption, and the capacity to support numerous connected devices. By adopting more specific technologies like LoRaWAN, Sigfox, and NB-IoT [Kadusic et al. 2022], LPWAN networks provide a robust and efficient infrastructure for communication across wide geographical areas.

Among LPWAN technologies, LoRaWAN has gained prominence due to its open-source standard and low deployment costs. Its architecture incorporates Long Range (LoRa) radio technology in the physical layer, enabling an extended signal range and deployment capability in both urban and rural areas. Thus, adopting the LoRaWAN specification offers several advantages, such as prolonged device battery life and extensive geographical coverage [Bonilla et al. 2023].

Furthermore, LoRaWAN networks must meet specific Quality of Service (QoS) requirements, which depends, among other factors, on the appropriate adjustment of specific transmission parameters, namely: Spreading Factor (SF), Transmission Power (TP), Bandwidth (BW), Coding Rate (CR), and Carrier Frequency (CF). This adjustment can be dynamically performed by a mechanism known as Adaptive Data Rate (ADR), which controls the transmission parameters of end devices to maximize network throughput and minimize energy consumption [Kufakunesu et al. 2020]. However, the efficacy of ADR is affected by a high configuration convergence period due to its conservative approach, gradually adapting transmission parameters values. This strategy is suitable for a static node environment but becomes unfeasible when there are variations in channel conditions [Farhad and Pyun 2022], resulting in degraded performance in scenarios involving mobile nodes, for instance.

Addressing this issue, alternative mechanisms to standard ADR have been proposed applying algebraic and statistical techniques, such as mean value [Slabicki et al. 2018], Gaussian filter [Farhad et al. 2020], and spatio-temporal correlation [Jiang et al. 2023], aiming to explore heuristics for handling frequent variations in channel conditions. Thus, this study proposes an alternative to standard ADR mechanism. The scheme named Percentile based ADR (P-ADR) employs percentile concepts [Amarnath Nandy and Ghosh 2022] to adjust appropriate signal-to-noise ratio (SNR) estimation values used in the ADR algorithm, effectively adapting to frequent changes in channel conditions and obtaining favorable Packet Delivery Ratio (PDR) values, a metric indicating the proportion of successfully transmitted packets relative to the total sent packets [Alahmadi et al. 2021].

Based on these premises, the main contributions of this paper are:

- Introduction of a viable alternative to standard ADR, showcasing satisfactory reliability performance, especially in scenarios involving mobile applications;
- Investigation of a statistical technique designed to alleviate the impact of SNR variability resulting from continuous changes in channel conditions;
- Provision of an easily implementable method for adjusting transmission parameters within LoRaWAN networks, necessitating minimal modifications on the network server side of ADR algorithm.

The remainder of this paper is organized as follows. Section 2 presents the theoretical background of this paper. Section 3 discusses the related works. Section 4 describes the proposed approach. The results obtained are detailed and discussed in Section 5. Finally, Section 6 concludes the paper with final remarks and directions for future work.

2. Theoretical Background

This section introduces LoRa and LoRaWAN technologies, emphasizing their key features and discussing the pertinent transmission parameters in LoRaWAN networks, as well as how the ADR mechanism operates to adjust them appropriately.

2.1. LoRa

The proprietary LoRa specification, developed by Semtech, addresses specific IoT requirements for LPWAN, focusing on long-range communication and low energy

consumption. This standard was designed to operate in unlicensed sub-GHz ISM (Industrial, Scientific, and Medical) bands, allocated according to the operating region [Ertürk et al. 2019].

Aiming to fulfill these requirements, LoRa implements Chirp Spread Spectrum (CSS) modulation, enabling devices to transmit at low data rates with long range, approximately 2 to 5 km in urban areas and 10 to 15 km in rural areas [Singh et al. 2023]. However, it is important to note that these distances can vary significantly depending on environmental conditions and interferences.

Moreover, LoRa transmission incorporates the Forward Error Correction (FEC) technique, enabling the use of redundant bits to aid in error detection and correction within frames. These combined features provide robust communication, more resilient to interference, making LoRa an attractive and cost-effective choice for LPWAN IoT communication applications [Kufakunesu et al. 2020].

2.2. LoRaWAN

The LoRaWAN specification, standardized by the LoRa Alliance, implements an open-source MAC protocol operating above the LoRa physical layer. This protocol facilitates data transmission from multiple devices while ensuring security and energy efficiency [Sadhu et al. 2022].

A typical LoRaWAN network adopts a star-of-stars topology, comprising End Devices (EDs), one or more Gateways (GWs), a Network Server (NS), and an Application Server (AS), as depicted in Figure 1. The EDs are responsible for collecting data or operating within a defined environment, sending and receiving packets. The GWs receive data packets from the EDs and forwards them to the NS using another communication technology, typically IP-based. Finally, the NS processes the received data and directs it to a specific AS for further processing and analysis [Kufakunesu et al. 2020].

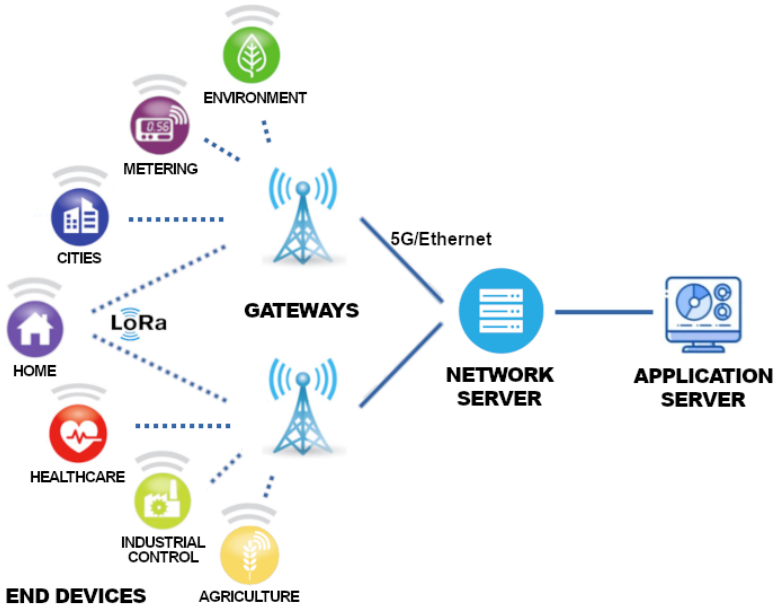

Figure 1. LoRaWAN network architecture.

Furthermore, LoRaWAN uses ALOHA as channel access protocol, which, although efficient in terms of simplicity, can lead to collisions when multiple EDs attempt simultaneous transmissions on the same channel [Picard et al. 2021]. One approach to mitigate these issues is by adjusting the transmission parameters within the LoRaWAN network. This adjustment allows devices, for instance, to communicate on different frequency spectrums, thereby reducing the likelihood of collisions.

2.3. Transmission Parameters

The communication between ED and GW involves several parameters that define fundamental settings for the operation of a LoRaWAN network. Some of these parameters are fine-tuned by the ADR mechanism, others can be adjusted under certain network conditions, and some are dependent on external factors, such as duty cycle limitations [Finnegan et al. 2020].

Spreading Factor represents the number of bits used in LoRa CSS modulation, more precisely determining the duration of a chirp, ranging between 2^7 (SF7) and 2^{12} (SF12) [Jouhari et al. 2023]. SF levels influence several transmission factors that bring trade-offs among them. For instance, lower SF values enhance the bit rate but reduce the communication range. To overcome this effect, higher SF values are used, enhancing SNR, allowing for extended-range communication. However, higher SF levels result in a longer Time on Air (ToA), the period during which the device is active for transmission, leading to a reduction in battery life due to prolonged radio transceiver activity [Moraes et al. 2022]. Furthermore, this parameter exhibit orthogonality, implying that modulated signals with different SF values, transmitted simultaneously on the same frequency channel, do not interfere with each other [Caillouet et al. 2019].

Transmission Power refers to the signal intensity emitted by a LoRa device, determining its reach and ability to penetrate obstacles or overcome interference conditions. Augmenting the TP can expand the signal range but escalates energy consumption. In its turn, Bandwidth is a parameter related to the amount of the spectrum portion used for transmission. Increasing the BW, for instance, from 125 kHz to 250 kHz [Kufakunesu et al. 2020], enables simultaneous transmission of a larger byte volume but it also makes the channel more susceptible to noise.

Another parameter is the Coding Rate, which is attached to FEC technique aforementioned and related to the redundancy of transmitted data, affecting resistance to interference and communication errors. Higher CR levels increase fault tolerance but also raise ToA and energy consumption [Ertürk et al. 2019]. Finally, the Carrier Frequency determines the central frequency of the communication channel. The selection of this parameter is attached to the operating region of the network, which adheres to regulations dictating the permissible ISM bands for usage.

In general, all these parameters have a direct impact on the QoS of LoRaWAN networks. The value of these factors can be determined statically by the network operator or dynamically by enabling the ADR mechanism on the network server. An important point to highlight is that the optimized adjustment of these parameters, when feasible, is essential to ensure transmission efficiency in LoRaWAN networks, finding the ideal balance between communication range, energy consumption, and reliability [Farhad and Pyun 2022].

2.4. Adaptive Data Rate

Considered as a key mechanism in LoRaWAN networks, Adaptive Data Rate enables the NS to control data rate, transmission power, channels used, and the number of retransmissions made by each ED in the network when sending packets. Using the SNR values from messages originating from an ED, the NS determines the proximity of that device to the nearest GW. This allows the NS to select the most suitable settings for each ED. The benefits of ADR are noteworthy, as it contributes to preserving the battery life of an ED and reducing communication interference [Jouhari et al. 2023].

ADR operates in two distinct parts: at the ED and at the NS. The NS implementation covers the more complex part, leaving the ED with the simpler task [Anwar et al. 2021]. The objective of the portion executed at the ED is simply to decrease the data rate to increase radio coverage if the uplink transmission does not reach the gateway (meaning loss of connection).

On the other hand, the portion executed in the NS facilitates the adjustment of TP and the increment of data rate for uplinks by decreasing SF. To achieve this, SNR values from received packets are collected by the server after ADR mechanism activation. Subsequently, based on Equations 1 and 2, the NS estimates the new SF and TP values for future transmissions until the subsequent ADR activation [Farhad et al. 2020]. According to Equation 1, when adjusted using the standard ADR, SNR_m stores the maximum SNR value based on the last $M = 20$ received packets. SNR_{req} stores the SNR value corresponding to the most recent packet, while $device_{margin}$ represents a signal tolerance constant, commonly set to $10\ dBm$ in various implementations [Slabicki et al. 2018][Ivoghlian et al. 2022]. In Equation 2, the value of N_{steps} determines the adjustment step for SF and TP values, communicated to the ED through $LinkADRReq$, a MAC command responsible for requesting changes to the values of the EDs configuration parameters. This iterative process enables the ADR to continuously optimize communication settings, dynamically adapting them for enhanced performance within the LoRaWAN network.

$$SNR_{margin} = SNR_m - SNR_{req} - device_{margin} \tag{1}$$

$$N_{steps} = floor(SNR_{margin}/3) \tag{2}$$

However, as previously mentioned, this SNR-based adjustment process is suitable for applications where nodes remain static, as ADR struggles to accommodate changes in channel conditions. For mobile EDs, Semtech recommends employing the Blind-ADR mechanism[1]. This method disregards channel conditions, opting instead for a temporal alternation among three spreading factor values (SF7, SF10, and SF12) to prioritize optimal communication coverage and energy efficiency, albeit potentially compromising PDR [Soy 2023].

[1]Blind-ADR. Retrieved January 02, 2024, from https://lora-developers.semtech.com/documentation/tech-papers-and-guides/blind-adr/

3. Related Work

This section outlines alternative solutions to the standard ADR mechanism in LoRaWAN networks. For a comprehensive overview, Table 1 provides a summary of the analysis of related works, focusing on the ability of the proposed methods to: i) adapt to scenarios involving mobile EDs, ii) mitigate the effects of SNR variability, and iii) be easily deployed with minimal modifications on both the ED and NS sides of the ADR mechanism.

Table 1. Comparing key aspects of P-ADR and related work.

	Method	*ED Mobility*	*SNR variability*	*Deployment*
[Slabicki et al. 2018]	ADR+	✓		✓
[Farhad et al. 2020]	G-ADR	✓	✓	
[Farhad et al. 2020]	EMA-ADR	✓	✓	
[Jiang et al. 2023]	K-ADR	✓	✓	
This work	P-ADR	✓	✓	✓

[Slabicki et al. 2018] modified the signal quality indication method by adopting the average SNR instead of the maximum SNR applied in the standard ADR. In a simulation considering urban and suburban scenarios, ADR+ presented by the mentioned study showed improvements in network reliability and energy efficiency compared to the standard ADR. However, despite ADR+ also applying statistical techniques to estimate the link quality indicator, the use of the average is not recommended in situations where data is skewed or contains outliers [Amarnath Nandy and Ghosh 2022], as is the case with SNR values obtained in LoRaWAN networks.

The limited responsiveness of ADR to fluctuating channel conditions and its prolonged configuration convergence time led [Farhad et al. 2020] to propose two solutions employing low-pass filters: Gaussian filter-based ADR (G-ADR) and Exponential Moving Average ADR (EMA-ADR). These methods aim to address rapid changes in the SNR of received packets at the NS, showcasing promising results in PDR and energy efficiency. Additionally, they showcase a reduction in the convergence time required for ADR adjustments, applicable to both stationary and mobile nodes. Nevertheless, G-ADR and EMA-ADR adjust SF and TP only when an $ADRACKReq$ MAC command with the ACK bit enabled is received, requiring ED to have ADR Backoff implementation [Finnegan et al. 2020], a feature available only in newer versions of the LoRaWAN specification.

In a recent development, [Jiang et al. 2023] introduced the K-ADR algorithm based on an Ordinary Kriging function, leveraging the spatiotemporal correlation of SNR to predict communication trends and anticipating the expected conditions for subsequent instances. Thus, K-ADR demonstrated PDR and energy consumption comparable to ADR+. However, the adopted simulation time is considered insufficient for a comprehensive analysis of the proposal, as it disregards the high configuration convergence time required by the ADR mechanism.

4. Proposed Approach

In scenarios characterized by frequent changes in channel conditions, the SNR values collected by the ADR scheme exhibit variations that interfere with the estimation

of new transmission parameter values. Under these conditions, adopting the maximum SNR value in the variable SNR_m, expressed in Equation 1, as an estimation factor for channel quality leads to slow adjustment convergence, resulting in a higher packet loss [Slabicki et al. 2018].

Aiming to determine the most representative value for the variable SNR_m, 400 sets of M SNR values were collected using the standard ADR mechanism, resulting in a total of 8000 samples. The analysis of this data distribution, depicted in the histogram presented in Figure 2(a), reveals an asymmetry, suggesting a higher concentration of data toward the lower end of the x-axis. The highest frequency of values, exceeding 1500 occurrences, can be noted between $-19\ dB$ and $-13\ dB$, indicating that lower SNR values are more common. The skewed nature of the distribution becomes more apparent when examining 20 random samples from the previously collected sets, as depicted in the boxplots shown in Figure 2(b). The elongated tails beyond the boxes and the frequent occurrence of outliers reinforce the high variability aspect of the data.

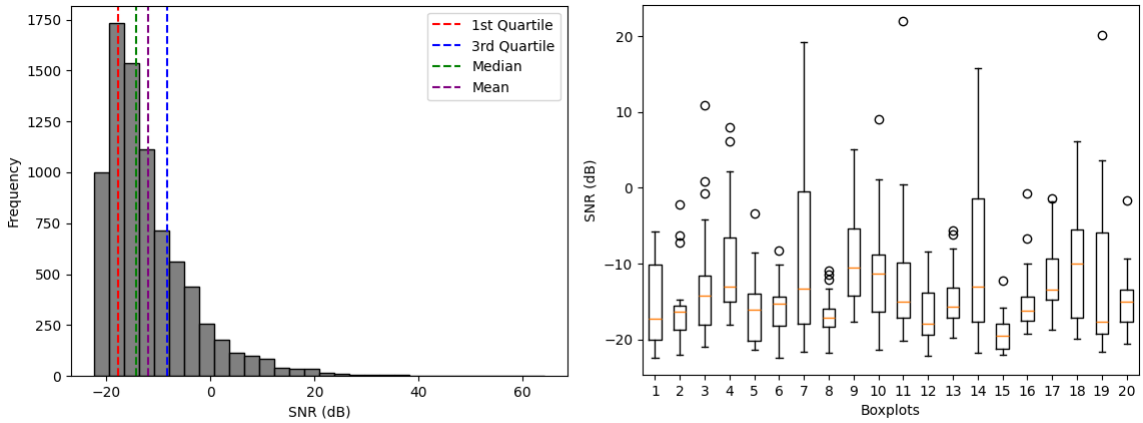

Figure 2. Distribution of SNR values using (a) histogram and (b) boxplots.

In such circumstances, assuming that the acquired SNR values are often subject to bias, utilizing maximum or mean values for estimating channel quality may result in suboptimal adjustments to network transmission parameters. Based on this premise, this study proposes an alternative approach to standard ADR by employing a percentile-based technique to mitigate the variability effect of SNR values [Amarnath Nandy and Ghosh 2022], as outlined in Algorithm 1. Initially, SNR_{list} is created to store the SNR values of the last $M = 20$ received packets, as shown in lines 1-3. Subsequently, the median and third quartile values, stored in the variables lb and ub respectively, are obtained, as indicated in lines 4-5. The average value of these variables then determines the new value for the variable SNR_m, as shown in line 6, which guides the algorithm through identical steps as the standard ADR, as described in lines 7-20.

Thus, P-ADR employs percentiles calculated from the gathered SNR values to estimate the variable SNR_m in order to mitigate the effects of channel state fluctuations. This method leads to an optimized adjustment of transmission parameters, enhancing reliability, particularly in scenarios involving mobile applications.

Algorithm 1: Proposed P-ADR scheme.

Input: $SF \in [7, 12],\ TP \in [2dBm, 14dBm], M, device_{margin}$

$SNRlist \leftarrow \emptyset$
for $i \leftarrow 0$ ***to*** $M - 1$ **do**
    $SNRlist[i] \leftarrow getSNR(i)$
$lb \leftarrow getMedian(SNRlist)$
$ub \leftarrow getThirdQuartile(SNRlist)$
$SNR_m \leftarrow (lb + ub)/2$
// Standard ADR Algorithm
$SNR_{req} \leftarrow demodulation\ floor\ (current\ data\ rate)$
$device_{margin} \leftarrow 10$
$SNR_{margin} \leftarrow SNR_m - SNR_{req} - device_{margin}$
$N_{steps} \leftarrow int\ (SNR_{margin}/3)$
while $N_{steps} > 0\ \ and\ \ SF > SF_{min}$ **do**
    $SF \leftarrow SF - 1$
    $N_{steps} \leftarrow N_{steps} - 1$
while $N_{steps} > 0\ \ and\ \ TP > TP_{min}$ **do**
    $TP \leftarrow TP - 2$
    $N_{steps} \leftarrow N_{steps} - 1$
while $N_{steps} < 0\ \ and\ \ TP < TP_{max}$ **do**
    $TP \leftarrow TP + 2$
    $N_{steps} \leftarrow N_{steps} + 1$
NS sends $LinkADRReq(SF,\ TP)$

5. Results and Discussion

This section outlines the experimental setup and the primary tools employed. Subsequently, the obtained results are presented and discussed.

5.1. Experimental Setup

In order to assess the performance of the proposed method, an experiment was conducted using Network Simulator[2] (NS-3) supplemented with the ELoRa module[3], which provides an updated implementation of the LoRaWAN specification [Aimi et al. 2023].

For a more comprehensive performance analysis, the experiment was designed to include: standard ADR, Blind ADR, and ADR+, methods based on statistical and algebraic techniques previously evaluated in related research [Slabicki et al. 2018] [Farhad and Pyun 2022]. Additionally, K-ADR was included to consider a recent proposal as an alternative to ADR [Jiang et al. 2023].

Drawing from realistic scenarios employed by [Farhad et al. 2020] [Anwar et al. 2021], the simulation entailed the deployment of Class A EDs uniformly distributed within a circular area of 5000 m radius, centered around a gateway, as illustrated in Figure 3. The EDs were subjected to a log-distance path loss model with

[2]NS-3. Retrieved January 02, 2024, from https://www.nsnam.org/releases/ns-3-40/
[3]ELoRa. Retrieved January 02, 2024, from https://github.com/Orange-OpenSource/elora

shadowing effect. To ensure a comprehensive analysis, scenarios involving both static and mobile EDs were encompassed. For the latter, a 2D random walk mobility model was employed, with device speeds ranging from 0.5 m/s to 1.5 m/s. All results are presented as average values based on 10 replications for each trial, utilizing distinct seeds for each replication. Table 2 outlines the key parameters employed in the simulation.

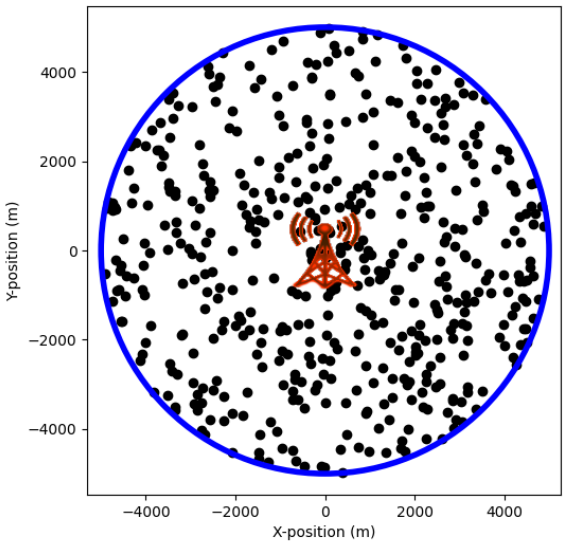

Figure 3. Static EDs positioning.

5.2. Analysis of Results

The primary indicator used to assess the effectiveness of the proposed solution is reliability. Figure 4 illustrates the average PDR across all evaluated methods while varying the number of EDs from 200 to 1000, in steps of 200. In Figure 4(a), considering only static EDs, there is no significant difference among the primary ADR methods. Remarkably, Blind-ADR does not integrate this comparison due to its significantly lower performance compared to the other solutions, owing to its simplistic SF assignment method disregarding channel conditions.

Table 2. Simulation Parameters.

Parameter	*Value (unit)*
Gateway radius	5000 m
Simulation time	4 days
App time period	144 packets/day
Packet size	30 bytes
Carrier frequency	868 MHz
Bandwidth	125 KHz
Code rate	4/8
Path loss exponent	3.76
Mobility model	2D Random Walk
ED movement speed	[0.5 , 1.5] m/s

Nevertheless, in Figure 4(b), depicting a scenario with mixed device mobility (50% static and 50% mobile EDs), the presence of partial mobility already demonstrates

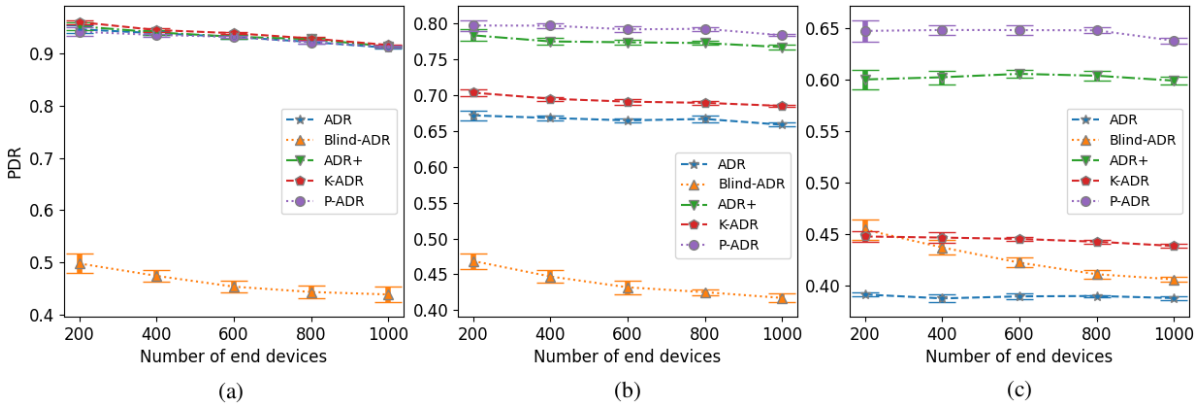

Figure 4. Average PDR for (a) static EDs, (b) mixed scenario (50% static and 50% mobile EDs) and (c) mobile EDs.

the prominence of P-ADR compared to other methods in trials involving 400 EDs and beyond. This is evident as there is no overlap of their respective 95% confidence intervals. When examining the overall average PDR of each method, calculated for the trials ranging from 200 to 1000 EDs, the difference between the proposed solution and the second-best solution (ADR+) is approximately 2%. However, when compared to the standard ADR, this difference amounts to approximately 12.5%.

In the case of complete mobility observed in Figure 4(c), the performance of the proposed solution exhibits an increase compared to other methods. The overall average difference between P-ADR and ADR+, under these conditions, is approximately 5%. Nevertheless, when compared to standard ADR, this difference exceeds 25%.

Considering a temporal scalability perspective of the PDR, as displayed in Figure 5, it becomes evident that all methods showcase a collective decrease in PDR levels, except for Blind-ADR, which exhibits an earlier decline due to employing a distinct configuration adjustment process. The overall decline observed in the other methods can be attributed to the common configuration convergence time, approximately 20 hours, inherent in all ADR-based solutions. This decline is associated with the impact of mobility in EDs [Farhad et al. 2020]. Among the examined solutions, ADR+ and P-ADR show the least susceptibility to this impact. Notably, the proposed solution demonstrates higher PDR values, particularly after 26 hours.

One of the main characteristics of LPWAN networks is energy efficiency. Thus, examining the results obtained regarding this aspect, Blind-ADR emerges as the most efficient solution, as evidenced in the graphs depicted in Figure 6. Irrespective of the mobility level, this method does not alter its average energy consumption curve. This behavior is justified by the logic of this scheme, which applies a temporal alternation among SF values without considering channel conditions. It is, therefore, a solution that prioritizes energy efficiency at the expense of reliability, as observed in Figure 4.

Upon further examination of the other solutions, in the context of scenarios involving solely static EDs, the average energy consumption values appear almost identical, as depicted in Figure 6(a). However, upon the introduction of mobility in the simulations, both ADR+ and P-ADR demonstrate marginally higher energy consumption compared to K-

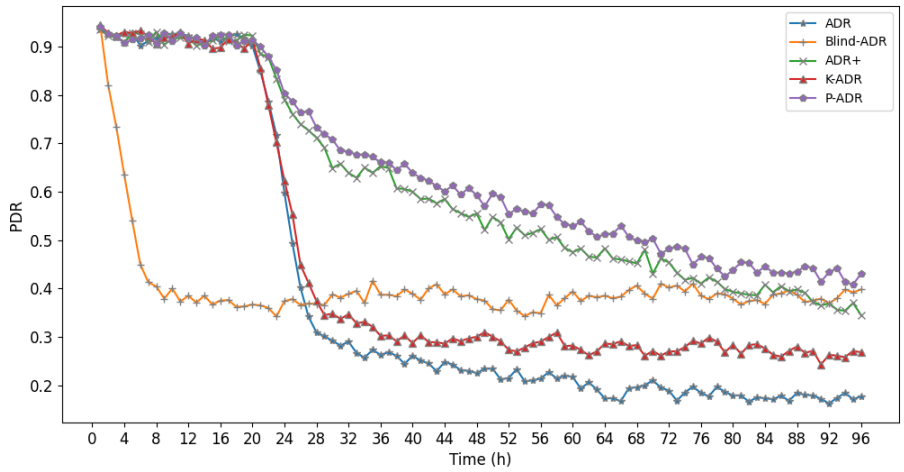

Figure 5. Average PDR over time for 1000 mobile EDs.

ADR and standard ADR. The differences among these methods become more pronounced in the mixed scenario. For instance, in a scenario involving 1000 EDs, the confidence interval difference between P-ADR and K-ADR amounts to approximately 1J, as depicted in Figure 6(b).

In contrast, when the ED mobility is total, as shown in Figure 6(c), the confidence intervals around the mean are larger compared to the previous scenarios, resulting in overlap for all considered methods. Thus, it is not possible to assert that there is a significant difference in average energy consumption among the solutions occupying the upper part of the graph. Consequently, P-ADR showcases an energy consumption level similar to the primary analyzed methods, except in comparison to Blind-ADR, which, as mentioned earlier, prioritizes energy efficiency over reliability.

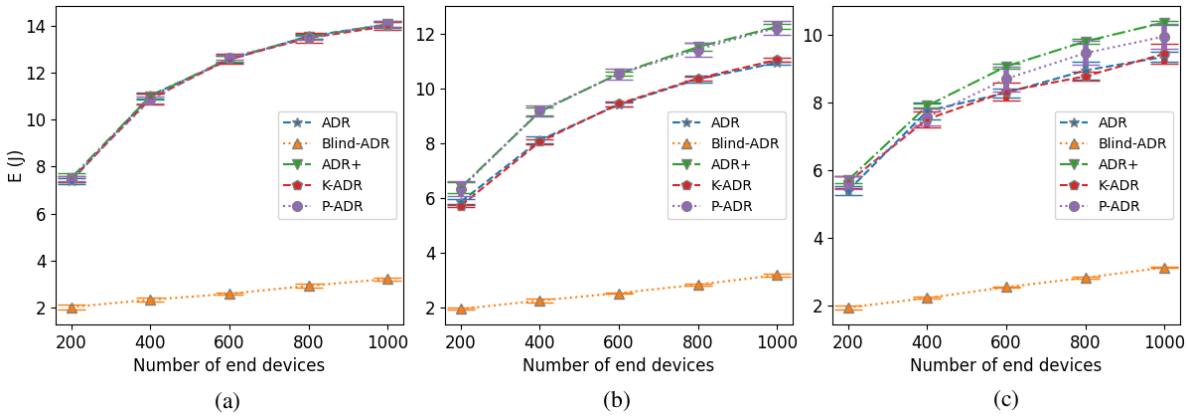

Figure 6. Average energy consumption (in J) for (a) static EDs, (b) mixed scenario (50% static and 50% mobile EDs) and (c) mobile EDs.

A notable observation arises upon analyzing these graphs, as shown in Figure 6: a discernible decline in the overall maximum energy consumption is evident on the y-axes as mobility rates increase. Since the energy consumption model used in NS-3 for Class A LoRa EDs only takes into account their transceiver activity, including transmission, reception windows, and idle state (i.e., sleep mode) [Finnegan et al. 2018], it does not take

into account the energy expended in device movement. Under these conditions, it can be inferred that mobile scenarios on average demand less power. This phenomenon might be attributed to the consistent alterations in channel conditions due to ED mobility, which alter the mutual interference between devices and subsequently impact the adjustment of the TP parameter within ADR methods.

Part of the energy consumption can also be justified by the SF values assigned to the EDs by the NS. As discussed in Section 2.3, the higher the SF value, the more ToA is required for bit transmission, resulting in higher energy consumption. Based on this premise, a certain pattern can be observed in Table 3, where in the scenario for 1000 mobile EDs, the average values of each SF for ADR and K-ADR are very close, reflecting the similarity of the curves of these methods shown in Figure 6(c). The average values of ADR+ and P-ADR also exhibit a certain proximity, which is also reflected in the energy consumption of these methods.

Among the evaluated solutions, Blind-ADR exhibits the lowest average assignment to the higher SF levels: 14.19%, considering the sum of SF11 and SF12 levels. In contrast, the other methods demonstrate higher values in the sum of those same levels: 25.53% for standard ADR, 25.46% for K-ADR, 50.14% for ADR+, and 55.63% for P-ADR. These data not only contribute to understanding energy consumption but also elucidate the average PDR obtained as a greater variability in SF values contributes to the mitigation of inter-SF interference [Caillouet et al. 2019], one of the factors responsible for packet loss in the network.

Table 3. Average SF assignment percentage for 1000 mobile EDs.

Method	*Spreading Factor (%)*					
	SF7	*SF8*	*SF9*	*SF10*	*SF11*	*SF12*
Blind-ADR	55.64	0	0	30.17	0	14.19
ADR	64.54	4.35	3.24	2.34	1.21	24.32
K-ADR	64.39	4.59	3.36	2.20	1.15	24.31
ADR+	17.01	8.74	12.01	12.10	16.00	34.14
P-ADR	11.05	8.93	11.36	13.03	18.46	37.17

Given the aforementioned, concerning energy consumption, P-ADR exhibited a disadvantage only when the average values obtained in the simulation were compared with Blind-ADR. However, the latter method demonstrates a severe PDR loss, making it a solution that could be adopted, for instance, in scenarios with low ED density or a low data transmission rate, particularly when device battery life constraints are more critical.

Nonetheless, P-ADR demonstrated an overall satisfactory performance concerning reliability and maintained a similar energy consumption level when compared to most of the considered solutions. This performance becomes more noticeable in scenarios involving mobile applications. This superiority is attributed to its estimation of the variable SNR_m based on percentiles, which proved to adapt more effectively to changes in channel conditions experienced in these scenarios.

6. Conclusion and Future Works

Embedded within LoRaWAN networks, the ADR mechanism dynamically adjusts transmission parameters to enhance the battery life of EDs and minimize communication

interference. However, this mechanism converges slowly to a suitable configuration, making it unrecommended for scenarios with signal fluctuations, such as in mobile applications. To overcome this limitation, a mechanism called P-ADR has been proposed. This algorithm utilizes percentiles to estimate channel quality, aiming to mitigate the effect of SNR variability caused by continuous changes in channel conditions.

Through simulation, the performance of the proposed solution was evaluated. The results demonstrated that P-ADR achieved a higher PDR compared to the standard ADR and other proposed solutions, including ADR+, K-ADR, and Blind-ADR. This superior performance was particularly evident in scenarios involving device mobility, showcasing an approximately 5% higher average PDR than ADR+ and an improvement of over 25% compared to the standard ADR.

Therefore, P-ADR represents a viable, easily deployable, and efficient alternative for dynamically adapting transmission parameters in LoRaWAN networks, offering a significant enhancement in reliability, especially in environments with mobile devices, without compromising network energy efficiency. As part of future work, conducting experiments with diverse network topologies and traffic scenarios, considering additional interference sources and deploying multiple gateways, could provide valuable insights. Additionally, further investigations can focus on implementing P-ADR in operational environments to evaluate its performance and behavior in real-use scenarios involving various IoT devices and applications.

References

Aimi, A., Rovedakis, S., Guillemin, F., and Secci, S. (2023). ELoRa: End-to-end Emulation of Massive IoT LoRaWAN Infrastructures. In *NOMS 2023-2023 IEEE/IFIP Network Operations and Management Symposium*, pages 1–3.

Alahmadi, H., Bouabdallah, F., Ghaleb, B., and Al-Dubai, A. (2021). Sensitivity-aware configurations for high packet generation rate LoRa networks. In *2021 20th International Conference on Ubiquitous Computing and Communications (IUCC/CIT/DSCI/SmartCNS)*, pages 240–246.

Amarnath Nandy, A. B. and Ghosh, A. (2022). Robust inference for skewed data in health sciences. *Journal of Applied Statistics*, 49(8):2093–2123.

Anwar, K., Rahman, T., Zeb, A., Khan, I., Zareei, M., and Vargas-Rosales, C. (2021). Rm-adr: Resource management adaptive data rate for mobile application in lorawan. *Sensors*, 21(23).

Bonilla, V., Campoverde, B., and Yoo, S. G. (2023). A systematic literature review of LoRaWAN: Sensors and applications. *Sensors*, 23(20).

Caillouet, C., Heusse, M., and Rousseau, F. (2019). Optimal SF allocation in LoRaWAN considering physical capture and imperfect orthogonality. In *2019 IEEE Global Communications Conference (GLOBECOM)*, pages 1–6.

Ertürk, M. A., Aydin, M. A., Büyükakkaşlar, M. T., and Evirgen, H. (2019). A Survey on LoRaWAN Architecture, Protocol and Technologies. *Future Internet*, 11(10).

Farhad, A., Kim, D.-H., Subedi, S., and Pyun, J.-Y. (2020). Enhanced LoRaWAN Adaptive Data Rate for Mobile Internet of Things devices. *Sensors*, 20(22).

Farhad, A. and Pyun, J.-Y. (2022). HADR: A Hybrid Adaptive Data Rate in LoRaWAN for Internet of Things. *ICT Express*, 8(2):283–289.

Finnegan, J., Brown, S., and Farrell, R. (2018). Modeling the energy consumption of LoRaWAN in ns-3 based on real world measurements. In *2018 Global Information Infrastructure and Networking Symposium (GIIS)*, pages 1–4.

Finnegan, J., Farrell, R., and Brown, S. (2020). Analysis and enhancement of the LoRaWAN Adaptive Data Rate scheme. *IEEE Internet of Things Journal*, 7(8):7171–7180.

Ivoghlian, A., Wang, K. I.-K., and Salcic, Z. (2022). Application-aware adaptive parameter control for LoRaWAN. *Journal of Parallel and Distributed Computing*, 166:166–177.

Jiang, Y., Wang, M., and Wang, X. (2023). A efficient Adaptive Data Rate algorithm in LoRaWAN networks: K-ADR. In *2023 24st Asia-Pacific Network Operations and Management Symposium (APNOMS)*, pages 183–188.

Jouhari, M., Saeed, N., Alouini, M.-S., and Amhoud, E. M. (2023). A survey on scalable LoRaWAN for massive IoT: Recent advances, potentials, and challenges. *IEEE Communications Surveys & Tutorials*, 25:1841–1876.

Kadusic, E., Ruland, C., Hadzajlic, N., and Zivic, N. (2022). The factors for choosing among NB-IoT, LoRaWAN, and Sigfox radio communication technologies for IoT networking. In *2022 International Conference on Connected Systems & Intelligence (CSI)*, pages 1–5.

Kufakunesu, R., Hancke, G. P., and Abu-Mahfouz, A. M. (2020). A survey on Adaptive Data Rate optimization in LoRaWAN: Recent solutions and major challenges. *Sensors*, 20(18).

Moraes, J., Oliveira, H., Cerqueira, E., Both, C., Zeadally, S., and Rosário, D. (2022). Evaluation of an adaptive resource allocation for LoRaWAN. *Journal of Signal Processing Systems*, 94(1):65–79.

Picard, A., Lapayre, J.-C., Hanna, F., and Muthada Pottayya, R. (2021). Comma: A new lorawan communication optimisation mechanism for mobility adaptation of iot. *IET Wireless Sensor Systems*, 11(3):120–130.

Sadhu, P. K., Yanambaka, V. P., and Abdelgawad, A. (2022). Internet of Things: Security and Solutions Survey. *Sensors*, 22(19).

Singh, S., Upaddhyay, V. K., and Soni, S. (2023). A literature review: LoRa technology and packet loss analysis in LoRaWAN line-up in our college campus. *Intelligent Systems and Smart Infrastructure: Proceedings of ICISSI 2022*, page 271.

Slabicki, M., Premsankar, G., and Francesco, M. D. (2018). Adaptive configuration of LoRa networks for dense IoT deployments. pages 1–9. IEEE.

Soy, H. (2023). An adaptive spreading factor allocation scheme for mobile LoRa networks: Blind ADR with distributed TDMA scheduling. *Simulation Modelling Practice and Theory*, 125:102755.